

Proof-Driven Clause Learning in Neural Network Verification

Omri Isac^{1*}, Idan Refaeli^{1*}, Haoze Wu², Clark Barrett³ and Guy Katz¹

¹ The Hebrew University of Jerusalem

² Amherst College

³ Stanford University

Abstract. The widespread adoption of deep neural networks (DNNs) requires efficient techniques for safety verification. Existing methods struggle to scale to real-world DNNs, and tremendous efforts are being put into improving their scalability. In this work, we propose an approach for improving the scalability of DNN verifiers using *Conflict-Driven Clause Learning* (CDCL) — an approach that has proven highly successful in SAT and SMT solving. We present a novel algorithm for deriving conflict clauses using UNSAT proofs, and propose several optimizations for expediting it. Our approach allows a modular integration of SAT solvers and DNN verifiers, and we implement it on top of an interface designed for this purpose. The evaluation of our implementation over several benchmarks suggests a $2\times$ – $3\times$ improvement over a similar approach, with specific cases outperforming the state of the art.

1 Introduction

Deep neural networks (DNNs) have made great strides in recent years, becoming the state-of-the-art solution for a variety of tasks in medicine [69], autonomous driving [18], natural language processing [67], and many other domains. However, DNNs lack structure that humans can readily interpret, rendering them opaque and potentially jeopardizing their reliability. One prominent example is the sensitivity of DNNs to small input perturbations, which can lead to significant and undesirable changes to the networks’ outputs. This sensitivity can be exploited maliciously [76], possibly leading to catastrophic results.

The pervasiveness of DNNs, combined with their potential vulnerability, has made DNN verification a growing research field within the verification community [3, 9, 10, 21, 22, 42, 49, 63, 68, 72, 75, 78, 79, 84]. Modern DNN verifiers typically make use of techniques such as SMT solving [1, 13, 29, 55], abstract interpretation [42, 63, 75, 80], LP solving [77], and combinations thereof. Many such verifiers are available [21, 22], and some tools have even been applied to industrial case studies [5, 36, 58]. Despite these achievements, DNN verifiers still scale only to medium-sized DNNs, with hundreds of thousands of neurons. As modern DNNs often contain millions of neurons and beyond, this issue restricts the applicability of DNN verifiers in real-world scenarios. Improving the scalability of DNN verification is thus the topic of much ongoing research.

* Both authors contributed equally

In this work, we contribute to these efforts, by focusing on the search procedure that is a component of many modern verifiers [63, 65, 77, 81]. As part of a search procedure, the DNN verifier typically casts the verification problem into a constraint satisfiability problem, and then traverses a large search space in search of an assignment to the DNN that satisfies the given constraints, consequently triggering undesirable behavior. Because this search space can be exponentially larger than the DNN, making the search more efficient (e.g., by curtailing the search space) can dramatically shorten verification times.

The search procedure within DNN verifiers resembles similar procedures applied in SAT and SMT solving, and we seek to improve it by applying tried and tested techniques from those domains. In particular, we focus on *Conflict-Driven Clause Learning* (CDCL) [16, 73, 74]. There, the search procedure identifies subspaces of the search space which are “similar” to subspaces already traversed, and which were shown not to contain any satisfying assignments. This similarity guarantees that the new subspaces also do not contain any satisfying assignments, and they can be safely skipped by the verifier. A core component in CDCL is the generation of *conflict clauses*: Boolean constraint clauses that are constructed whenever the search procedure encounters an unsatisfiable (UNSAT) subspace, and which guide the solver not to search in other subspaces that are also guaranteed to be UNSAT. Naturally, the algorithm for deriving conflict clauses is a key to a successful CDCL framework.

In the context of DNN verification, we propose to learn clauses using *UNSAT proofs* [50]. Whenever an UNSAT subspace of the problem is discovered, a proof of its unsatisfiability can be produced, and then used in learning a conflict clause. Towards this end, we developed a method that receives a proof of unsatisfiability and analyzes which neurons of the DNN participate in this proof. This analysis produces a set of *neuron phases* that are sufficient for refuting the existence of a satisfying assignment; and this set is then translated into a conflict clause. Our proposed analysis gives rise to nontrivial conflict clauses, which prune large subspaces of the search space. To the best of our knowledge, although initial attempts have been made to integrate CDCL principles into DNN verifiers [32, 33, 61], these attempts either use naive conflict clauses, or invoke time-consuming algorithms to minimize the conflict clauses’ sizes [23]. Our approach, on the contrary, leverages proofs of unsatisfiability and tends to produce clauses efficiently.

Building on the aforementioned principle, we propose a CDCL-based algorithm for verifying DNNs. We implemented our algorithm on top of the IPASIR-UP interface, which enables combining a state-of-the-art SAT solver [17, 39, 40] and DNN verifier [81]. We then applied our implementation to several benchmarks, including verification queries that involve neural activation patterns (NAPs) [43, 47]. On such queries, our tool outperforms even optimized verifiers.

Our contributions can be summarized as follows: (i) we present a novel algorithm for deriving conflict clauses from UNSAT proofs in DNN verification queries; (ii) we use this algorithm to implement a CDCL verification scheme based on a modern DNN verifier and SAT solver; (iii) we explore optimizations and heuristics to improve our scheme’s performance; and (iv) we demonstrate the perfor-

mance improvement of our method over a similar verifier, and the improvement over optimized verifiers for properties describing DNNs behavior via NAPs.

The rest of this paper is organized as follows: In Section 2 we provide the necessary background on DNNs and their verification, and on the use of proof production and CDCL in this context (we assume the reader is familiar with basic notions of propositional and first-order logic). In Section 3 we describe the algorithms used to develop our CDCL scheme for DNN verification and its optimizations. In Section 4 we discuss our implementation of these algorithms, and in Section 5 we provide an evaluation of our algorithm. Finally, in Section 6 we conclude, discuss related work, and outline directions for future research.

2 Background

2.1 DPLL and DPLL(\mathcal{T})

DPLL is a well-known algorithm for solving the satisfiability problem for propositional formulas (SAT) [27, 28], and lies at the foundation of modern SAT solvers. Without loss of generality, the algorithm operates on formulas in Conjunctive Normal Form (CNF), i.e, a conjunction of *clauses*, where each clause is comprised of a disjunction of *literals* — Boolean variables or their negations. Given a formula φ in CNF, the algorithm searches for a satisfying assignment to the variables, and returns **SAT** if it finds one or **UNSAT** if no such assignment exists.

The algorithm iteratively *decides* the assignment of a variable, attempts to *propagate* the assignment of additional variables, and repeats these steps until it either discovers a **SAT** assignment, or until it encounters a conflict and determines that the current trail of decisions is **UNSAT**. If a conflict is detected, the algorithm *analyses* it to determine the decisions that caused it. Then, the algorithm *backtracks* — it erases all variable assignments beyond the last decision that contributed to the conflict, reverses that decision, and continues. If at some point all variables are assigned without causing a conflict, a **SAT** assignment is found. Otherwise, if all possible decisions have been exhausted, the algorithm returns **UNSAT**. Each decision splits the query into two subqueries, essentially creating a search tree of Boolean assignments.

In *Satisfiability Modulo Theories (SMT)* [13], DPLL is extended into DPLL(\mathcal{T}) — an algorithm capable of determining the satisfiability of first-order formulas over given background theories [41]. The DPLL(\mathcal{T}) algorithm employs both a SAT solver to reason about a *Boolean abstraction* of a given formula, together with theory solvers (\mathcal{T} -solvers) to reason about the formula’s first-order components. Although DPLL(\mathcal{T}) solvers can support multiple \mathcal{T} -solvers [66], here we focus on the combination of a SAT solver with a single \mathcal{T} -solver.

To create the Boolean abstraction, the DPLL(\mathcal{T}) solver assigns a Boolean variable to each atom in the input formula φ .

The underlying SAT solver begins reasoning on this abstract Boolean formula, as in DPLL. When solving, the SAT solver occasionally invokes the \mathcal{T} -solver with the partial Boolean assignment it has discovered so far, allowing the \mathcal{T} -solver to perform propagations (\mathcal{T} -propagate) or report on conflict (\mathcal{T} -conflict) on the first-order constraints, similarly to how the SAT solver does this

for Boolean formulas. In addition, \mathcal{T} -solvers may be requested to *explain* past propagations they reported, i.e., to provide a conjunction of assigned literals sufficient to imply the propagation.

2.2 Deep Neural Networks and their Verification

Deep Neural Networks (DNNs) [46]. Formally, a DNN $\mathcal{N} : \mathbb{R}^n \rightarrow \mathbb{R}^m$ is a sequence of k layers L_0, \dots, L_{k-1} where each layer L_i consists of $s_i \in \mathbb{N}$ nodes $v_i^1, \dots, v_i^{s_i}$ and s_i biases $b_i^j \in \mathbb{Q}$. Each directed edge in the DNN is of the form (v_{i-1}^l, v_i^j) and is labeled with a weight $w_{i,j,l} \in \mathbb{Q}$. The assignment to the nodes in the input layer is defined by $v_0^j = x_j$, where $\bar{x} \in \mathbb{R}^n$ is the input vector, and the assignment for the j^{th} node in the $1 \leq i < k-1$ layer is computed as $v_i^j = f_i \left(\sum_{l=1}^{s_{i-1}} w_{i,j,l} \cdot v_{i-1}^l + b_i^j \right)$ for some activation function $f_i : \mathbb{R} \rightarrow \mathbb{R}$. Finally, neurons in the output layer are computed similarly, where f_{k-1} is the identity.

One common activation function is the *rectified linear unit* (ReLU), defined as $\text{ReLU}(x) = \max(x, 0)$. The function has two phases: if the input of the ReLU function is non-negative, the function is *active*; otherwise, the function is *inactive*. For simplicity, we focus on DNNs with ReLU activations, though our work can be extended to support any piecewise-linear activation (e.g., *maxpool*).

Example 1. A simple DNN with four layers appears in Figure 1. For simplicity, all biases are set to 0 and are omitted. For input $\langle 2, 1 \rangle$, the node in the second layer evaluates to $\text{ReLU}(2 \cdot 1 + 1 \cdot (-1)) = \text{ReLU}(1) = 1$; the nodes in the third layer evaluate to $\text{ReLU}(1 \cdot (-2)) = 0$ and $\text{ReLU}(1 \cdot 1) = 1$; and the node in the output layer evaluates to $0 + 1 \cdot 2 = 2$.

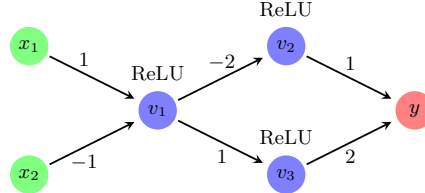


Fig. 1: A toy DNN with ReLU activations.

The DNN Verification Problem. Consider a trained DNN $\mathcal{N} : \mathbb{R}^n \rightarrow \mathbb{R}^m$ where $\bar{x} \in \mathbb{R}^n, \bar{y} \in \mathbb{R}^m$ denote the network's inputs and outputs. The *DNN verification problem* is the problem of deciding whether there exist $(\bar{x}, \bar{y}) \in \mathbb{R}^{n+m}$ such that $\bar{y} = \mathcal{N}(\bar{x}) \wedge \varphi_I(\bar{x}) \wedge \varphi_O(\bar{y})$ for some property $\varphi_I \wedge \varphi_O$. If such \bar{x}, \bar{y} exist, we say the problem is satisfiable, denoted **SAT**. Otherwise, we say that it is unsatisfiable, denoted **UNSAT**. In this work, we consider *quantifier-free, linear properties*, i.e., formulas whose atoms are linear equations and inequalities.

Example 2. Consider the DNN from Figure 1, and the property $\varphi_I(\bar{x}) := (1 \leq x_1) \wedge (1 \leq x_2) \wedge (x_1 \leq 2) \wedge (x_2 \leq 2)$, and $\varphi_O(y) := (y \leq -1)$. This instance is **UNSAT**, as the output is a sum of two non-negative components with positive weights.

Linear Programming (LP) [26] and DNN Verification. In LP we seek an assignment to a set of variables that satisfies a set of linear constraints, while maximizing a given objective function. As is common in the context of DNN verification, we assume here that the objective function is constant, and ignore it. Formally, let $V = [x_1, \dots, x_n]^T \in \mathbb{R}^n$ denote variables, $A \in M_{m \times n}(\mathbb{R})$ denote a constraint matrix and $l, u \in (\mathbb{R} \cup \{\pm\infty\})^n$ denote vectors of bounds. The LP problem is to decide the satisfiability of $(A \cdot V = 0) \wedge (l \leq V \leq u)$. Throughout the paper, we use $l(x_i)$ and $u(x_i)$, to refer to the lower and upper bounds (respectively) of x_i .

A DNN verification query can be encoded as a tuple $Q = \langle V, A, l, u, R \rangle$, where $\langle V, A, l, u \rangle$ constitute a linear program [26, 55] that represents the property and the affine transformations within \mathcal{N} , and where R is the set of ReLU activation constraints. Using this encoding, the verification query can be dispatched through a series of invocations of an LP solver, combined with *case splitting* to handle the piecewise-linear constraints [55]. Schematically, the DNN verifier begins by invoking the LP solver over the linear part of the query. An **UNSAT** result of the LP solver implies the overall query is **UNSAT**. Otherwise, the LP solver finds an assignment that satisfies the linear part of the query. If this assignment satisfies the piecewise-linear part of the query, the DNN verifier may conclude **SAT**. If neither case applies, the DNN verifier splits the query into two subqueries, by deciding the phase of a single ReLU constraint $f_i = \text{ReLU}(b_i)$. One subquery is augmented with the additional linear constraint $f_i - b_i = 0$ and the bound $b_i \geq 0$, corresponding to the active phase; the other is augmented with the constraints $b_i \leq 0$ and $f_i = 0$, corresponding to the inactive phase. Then, the LP solver is invoked again over each subquery, and the process repeats.

Example 3. We demonstrate this encoding with the example presented in Figure 1 and the property from Example 2. Let x_1, x_2 denote the network’s inputs and y denote its output, and let b_i, f_i ($i \in \{1, 2, 3\}$) denote the input and output of neuron v_i , respectively. The affine transformations of the network are reduced to the equations $x_1 - x_2 - b_1 = 0$, $2f_1 + b_2 = 0$, $f_1 - b_3 = 0$, and $f_2 + 2f_3 - y = 0$. The property is encoded using the inequalities $(1 \leq x_1)$, $(1 \leq x_2)$, $(x_1 \leq 2)$, $(x_2 \leq 2)$, and $(y \leq -1)$. We also add the inequalities $(0 \leq f_i)$ (for $i \in \{1, 2, 3\}$) to express the non-negativity of ReLUs. The aforementioned constraints form the LP part of the query; and its piecewise-linear portion is comprised of the constraints $f_i = \text{ReLU}(b_i)$ for $i \in \{1, 2, 3\}$.

This approach creates an abstract tree structure for the search, where each node represents a case split. If the LP solver deduces **UNSAT** for each leaf of the tree, then the original query is **UNSAT** as well. If not, then due to the completeness of LP solvers, it finds a satisfying assignment for one of the subqueries.

The search tree may be exponentially large in the number of neurons. Therefore, it is very common to use case splitting as rarely as possible, and apply algorithms to deduce tighter bounds of variables. These algorithms may conclude in advance that some neurons’ phases are fixed, i.e., they are always active or always inactive, thus avoiding the need to split on these neurons.

The Marabou Verifier. For our evaluation, we used the Marabou verifier — a state-of-the-art framework for DNN verification [56, 81]. When solving a

verification query, Marabou employs customized search-based techniques [83], together with modern bound tightening approaches [63]. Marabou has been used for a range of case-studies, e.g., from the domains of robotics [4, 14], computer networks [7, 38, 57], and aerospace [36]; and for varied tasks, such as ensemble selection [8], generalizability testing [6], network pruning [44, 59], formal explainability [15], and repair [45, 71]. In addition, Marabou has been enhanced with abstraction-refinement capabilities, to further improve its scalability [25, 34, 35, 37].

2.3 Proof Production for DNN Verification

When DNN verification is regarded as a satisfiability problem, a satisfying assignment is an efficient proof of **SAT**: one can simply run it through the network and observe that it satisfies the property in question. The **UNSAT** case is more complex, and requires producing a *proof certificate*. The first method for proof production in DNN verification performed via LP solving and case splitting was introduced in [50]. The proof certificates produced therein consist of a *proof tree* that replicates the search tree created by the verifier, and is constructed during the verification process. Recall that for an **UNSAT** query, all leaves of the search tree represent **UNSAT** subqueries. Therefore, each internal node of the proof tree represents a case split performed by the verifier, and each leaf corresponds to a subquery for which the verifier has deduced **UNSAT**.

In each leaf of the search tree, the verifier was able to conclude **UNSAT** using solely the available linear constraints. Thus, a proof for the leaf’s unsatisfiability can be described as a vector, according to the Farkas lemma [24], which combines the linear constraints to derive an evident contradiction [50].

More formally:

Theorem 1 (Farkas Lemma Variant (From [50])). *Observe the constraints $A \cdot V = \bar{0}$ and $l \leq V \leq u$, where $A \in M_{m \times n}(\mathbb{R})$ and $l, V, u \in \mathbb{R}^n$. The constraints are **UNSAT** if and only if $\exists w \in \mathbb{R}^m$ such that for $w^\top \cdot A \cdot V := \sum_{i=1}^n c_i \cdot x_i$, we have that $\sum_{c_i > 0} c_i \cdot u(x_i) + \sum_{c_i < 0} c_i \cdot l(x_i) < 0$ whereas $w^\top \cdot \bar{0} = 0$. Thus, w is a proof of the constraints’ unsatisfiability, and can be constructed during LP solving.*

Example 4. We demonstrate this theorem with our example. Consider the query based on the DNN in Figure 1 and the property in Example 2. Assume, for simplicity, that all lower and upper bounds not explicitly stated are -1 or 1 , respectively. Further assume that both v_2, v_3 are inactive (i.e. $f_2 = f_3 = 0$ and $b_2, b_3 \leq 0$). The linear part of the query yields the LP:

$$A = \begin{bmatrix} 1 & -1 & -1 & 0 & 0 & 0 & 0 & 0 & 0 \\ 0 & 0 & 0 & 1 & 0 & 2 & 0 & 0 & 0 \\ 0 & 0 & 0 & 0 & -1 & 1 & 0 & 0 & 0 \\ 0 & 0 & 0 & 0 & 0 & 0 & 1 & 2 & -1 \end{bmatrix} \quad \begin{aligned} u &= [2 \ 2 \ 1 \ 0 \ 0 \ 1 \ 0 \ 0 \ -1]^\top \\ V &= [x_1 \ x_2 \ b_1 \ b_2 \ b_3 \ f_1 \ f_2 \ f_3 \ y]^\top \\ l &= [1 \ 1 \ -1 \ -1 \ -1 \ 0 \ 0 \ 0 \ -1]^\top \end{aligned}$$

Consider now the vector $w = [0 \ 0 \ -1 \ -2]^\top$. The product $w^\top \cdot A \cdot V$ yields the equation $-f_1 + b_3 - 2f_2 - 4f_3 + 2y = 0$. The left hand side of the equation is at

most $-l(f_1) + u(b_3) - 2 \cdot l(f_2) - 4 \cdot l(f_3) + 2 \cdot u(y) = -2 < 0$. Therefore, according to Theorem 1, w is a proof of UNSAT. Note that there may be multiple proofs of this result. An overall proof of UNSAT for the query consists of a proof tree, where each leaf has a proof vector proving UNSAT for the corresponding subquery.

Bound Tightening Lemmas. DNN verifiers often employ bound tightening procedures that deduce bounds using the non-linear activations. In general, each bound tightening lemma consists of a ground bound and a learned bound, which replaces a bound currently in l or u . Such lemmas generally cannot be captured by the Farkas vector, and require separate proofs. For example, given $f = \text{ReLU}(b)$ and present bounds $f \leq 5$ and $b \leq 7$, it is possible to deduce that $b \leq 5$. To prove such a lemma, we would use a Farkas vector that proves $f \leq 5$, and apply to it another proof rule that captures this form of bound derivation.

Example 5. Consider the query Q in Example 4. We can use the equation $b_2 = -2f_1$, which is equivalent to $2f_1 + b_2 = 0$, to deduce that $u(b_2) = -2 \cdot l(f_1) = 0$. Then, based on the ReLU constraint, we deduce that the neuron v_2 is inactive, i.e., that $u(f_2) = 0$. A lemma with a ground bound $u(b_2) = 0$, learned bound $u(f_2) = 0$ and a proof vector for generating $b_2 = -2f_1$ (the vector $[0 \ -1 \ 0 \ 0]^\top$) is learned at the root of the proof tree, without any case splits. Similarly, we can deduce that v_3 is inactive by learning a lemma with a ground bound $u(f_3) = -0.5$, learned bound $u(b_3) = 0$ and a proof vector $[0 \ 0 \ 0 \ -0.5]^\top$. Combined with Example 4, we get a proof of UNSAT for Q that consists of a single node with two lemmas, as illustrated in Figure 2.

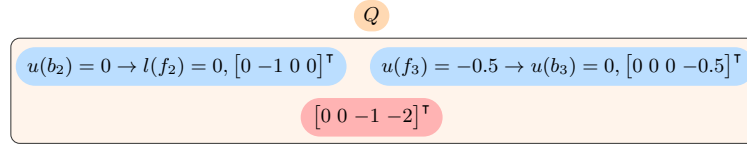


Fig. 2: A proof tree example with a single node (orange). Given the query Q , two lemmas (blue) are learned, and used to derive UNSAT (red).

3 Conflict-Driven Clause Learning for DNN Verification

3.1 DNN Verifiers as \mathcal{T} -Solvers

The DNN verification problem can be formulated as an SMT problem, where an underlying SAT solver deals with the case splitting, and a single theory solver, for the theory of linear real arithmetic, deals with linear constraints. Separating the Boolean- and theory-specific reasoning in this way, as is generally done in SMT solving, is beneficial for multiple reasons: (i) it provides a clean logical separation of these two distinct levels of reasoning; (ii) it enables a modular integration of modern SAT solvers into DNN verifiers, allowing the DNN verifier to benefit from advances in SAT solving; (iii) it often allows for more expedient solving times; and (iv) it paves the way for future integration with additional theory solvers. Despite these facts, most modern DNN solvers do not follow this architecture.

Instead, they either mix the two layers completely, or separate them entirely, so that very little information flows between the two. Here, we advocate leveraging the knowledge and experience gained by the SMT community in the recent decades, by designing a DNN verifier according to the DPLL(\mathcal{T}) architecture.

Indeed, initial attempts have been made to design DNN verifiers according to the DPLL(\mathcal{T}) architecture [32, 33, 55, 61]. Here we take the next step, and present a CDCL(\mathcal{T})-based DNN verifier. Conflict-Driven Clause Learning (CDCL) [16, 73, 74] enhances DPLL by adding learned conflict clauses to the formula being solved. Each such clause represents the negation of a partial assignment that caused unsatisfiability, and is hence implied by the original formula. The usefulness of such a clause is that it prevents the solver from revisiting a similar subspace of the search space, which is guaranteed to contain no satisfying assignments. When used within a SAT solver, CDCL will often significantly prune the resulting search tree, improving scalability considerably [16, 73, 74]. SMT solvers extensively use CDCL(\mathcal{T}), the first order extension of CDCL [13].

To facilitate the design of a DNN verifier as a CDCL(\mathcal{T}) solver, we follow previous work [32, 33, 61] and use Boolean reasoning over the *neurons* of the DNN, i.e., the linear phases of the activation functions. Therefore, unlike general-purpose SMT solvers, only a subset of the theory constraints (namely, the phases of the activation functions) are represented as Boolean variables, whereas the remaining constraints are internal to the \mathcal{T} -solver.

Using this Boolean abstraction, the CDCL-based solver that we propose consists of two main components:

(1) a SAT solver, for reasoning about the neuron activation phases; and (2) a DNN theory solver for reasoning about the linear constraints imposed by these phases. Each neuron in the DNN \mathcal{N} is assigned an index i , and an “abstract” Boolean variable X_i . Initially, the SAT solver receives the trivial Boolean formula $\bigwedge_{i \in |\mathcal{N}|} (X_i \vee \neg X_i)$, indicating that each (ReLU) activation function must be either active or inactive. (Throughout this paper, we use lower-cased variables to denote first-order variables, and upper-cased variables to denote Boolean variables). The DNN verifier receives the verification query as before (including the input and output constraints). In Section 3.3 we explore properties expressed using additional clauses added to the SAT solver.

In our algorithm, the SAT solver is responsible for performing decisions, propagations based on Boolean reasoning, and backtracking, all of which can be carried out at the Boolean abstraction level. In addition, the DNN verifier may deduce facts that need to be translated to Boolean level. The extensive use of bound tightening, for example, may be used to deduce phase-fixing bounds as in Example 5. Whenever an active (inactive) phase of a neuron i is deduced, the boolean literal X_i ($\neg X_i$) is propagated to the SAT solver. Whenever the DNN verifier concludes a partial assignment is **UNSAT**, it is requested to provide a conflict clause. Naively, the verifier may provide the partial assignment as a clause; but we later show how **UNSAT** proofs can be used to derive nontrivial, more effective clauses. If the DNN verifier concludes that the complete assignment is **SAT**, then so is the overall query.

Example 6. Consider the query presented in Example 4. It consists of a linear part and a list of piecewise-linear constraints. Each constraint $f_i = \text{ReLU}(b_i)$ is abstracted to the Boolean variable X_i , resulting in the query depicted in Figure 3.

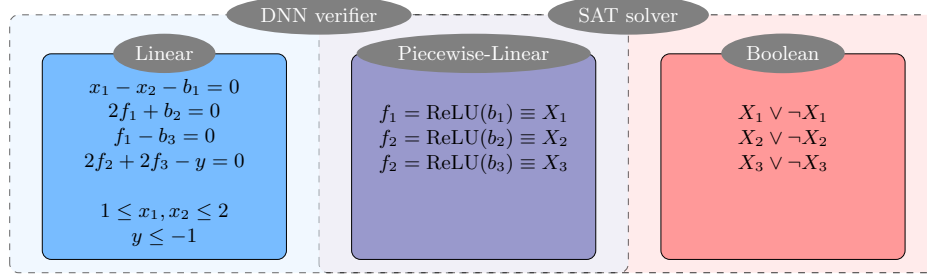


Fig. 3: An example of a query comprised of linear constraints, piecewise-linear constraints, and the Boolean abstraction.

In case the DNN verifier deduces the lemma as in Example 5, it can be propagated to the SAT solver as $\neg X_2$. Since this lemma is valid (i.e., does not depend on past splits), its explanation is simply $\neg X_2$.

3.2 Conflict Deduction with Proofs

We next discuss how UNSAT proofs can be used to deduce conflict clauses. The core idea is to analyze, for each proof vector as in Theorem 1, the set of neurons whose activation phases *participate* in the proof; that is, phases sufficient to deduce UNSAT using the proof.

For simplicity, we first assume that no bound tightening lemmas are learned. Consider a proof vector w that proves UNSAT for some proof-tree leaf within a DNN verification query $Q = \langle V, A, l, u, R \rangle$. Furthermore, consider α , a partial assignment of the Boolean variables that represents the UNSAT leaf. According to Theorem 1, w is certified using a subset of A rows, ignoring rows whose coefficients in w are zero; and a subset of the bounds, $\sum_{c_i > 0} c_i \cdot u(x_i) + \sum_{c_i < 0} c_i \cdot l(x_i)$,

where variables with zero coefficients are ignored. In other words, the lower bounds of all x_i with $c_i < 0$, and the upper bounds of all x_i with $c_i > 0$, are sufficient conditions to derive UNSAT using w . In the absence of bound tightening lemmas, all bounds that are used to update l and u originated from splitting over ReLU constraints. This gives rise to Algorithm 1, which derives such sufficient constraints given w , and returns their corresponding (abstract) Boolean clause.

Algorithm 1 iterates through the ReLU constraints of the query. For each ReLU, it checks whether its phase is fixed, and whether the linear constraints derived from the phase participate in the refutation. If so, the Boolean abstraction of the phase is added to the conjunction of constraints implying UNSAT. After checking all ReLU constraints, C contains a subset of constraints sufficient to imply a contradiction, and is negated to deduce a conflict clause.

Example 7. In Example 4, the vector $w = [0 \ 0 \ -1 \ -2]^\top$ is used to derive UNSAT, by computing $w^\top \cdot A \cdot V = -f_1 + b_3 - 2f_2 - 4f_3 + 2y$. To deduce UNSAT, we used

Algorithm 1 *proofCC'()*: Conflict clause from UNSAT proofs, w/o lemmas

Input: A DNN verification query $Q = \langle V, A, l, u, R \rangle$, an UNSAT partial assignment α , and a proof vector w

Output: A conflict clause of boolean variables

```

    // Let  $\sum_{i=1}^n c_i \cdot x_i$  denote the linear combination of variables in  $w^\top \cdot A \cdot V$ 
1:  $C := \emptyset$  ▷ The conflict clause
2: for  $X_j \in R$  do
3:    $x_{j_1} := b_j, x_{j_2} := f_j$  ▷ The input and output of ReLUj, respectively
   // Let  $f_j - b_j = 0$  denote the  $k^{th}$  row of  $A$ 
4:   if  $\alpha(X_j) = \top$  then ▷ ReLUj is active
5:     if  $c_{j_1} < 0$  or  $w_k \neq 0$  then ▷ Check participation in the contradiction
6:        $C := C \wedge X_j$ 
7:     end if
8:   else if  $\alpha(X_j) = \perp$  then ▷ ReLUj is inactive
9:     if  $c_{j_1} > 0$  or  $c_{j_2} > 0$  then ▷ Check participation in the contradiction
10:       $C := C \wedge \neg X_j$ 
11:    end if
12:  end if
13: end for
14: return  $\neg C$ 

```

the upper bound of b_3 , which is equal to 0 — implying that ReLU₃ is inactive (the lower bounds of f_1, f_2, f_3 are used as well, but they all equal 0 regardless of the phase). Therefore the single literal $\neg X_3$ is sufficient for proving UNSAT with w , and the conflict clause X_3 is learned. Note that although ReLU₂ was inactive when deducing UNSAT using w , it is unnecessary for the deduction, and thus the corresponding negated literal X_2 is not included in the conflict clause.

Bound tightening lemmas, when introduced, need to be considered in the analysis as well. We distinguish between two types of lemmas: (i) phase-fixing lemmas, which are used to fix the phase of some ReLU constraint, such as in Example 5; and (ii) non-phase-fixing lemmas, which are used to learn bounds without fixing any phase. Phase-fixing lemmas can be represented with a Boolean literal, and we can address them by adding the representing literal to the clause. Whenever a contradiction is dependent on a phase-fixing lemma, the literal becomes part of the assignment α and is thus checked during the loop of Algorithm 1. This requires implementing \mathcal{T} -explain for these literals, as they are deduced by the DNN verifier. We return to \mathcal{T} -explain later in this section. Non-phase-fixing lemmas, however, require a different approach.

To properly support all bound tightening lemmas, we present Algorithm 2, which can deduce the lemma dependency of each proof vector. To do so, we store for every bound $l(x_i), u(x_i)$, the lemma that was used to deduce it. Then, we can collect the lemmas that deduce all non-zero entries of $\sum_{c_i > 0} c_i \cdot u(x_i) + \sum_{c_i < 0} c_i \cdot l(x_i)$.

Recall that each lemma has its own proof, which could be used to analyze their dependencies.

Algorithm 2 *proofLemmas()*: Lemma dependency of UNSAT proofs

Input: A DNN verification query $Q = \langle V, A, l, u, R \rangle$, a list of lemmas Lem , and a proof of UNSAT w

Output: A list of lemmas sufficient to deduce UNSAT

```
// Let  $\sum_{i=1}^n c_i \cdot x_i$  denote the linear combination of variables in  $w^\top \cdot A \cdot V$ 
1:  $L := \emptyset$  ▷ An empty list of lemmas
2: for  $i \in [n]$  do
3:   if  $c_i > 0$  and  $u(x_i)$  is learned by a non-phase-fixing lemma  $l_i^u \in Lem$  then
4:      $L := L \cup l_i^u$ 
5:   else if  $c_i < 0$  and  $l(x_i)$  is learned by a non-phase-fixing lemma  $l_i^l \in Lem$  then
6:      $L := L \cup l_i^l$ 
7:   end if
8: end for
9: return  $L$ 
```

Algorithm 3 *proofCC()*: Conflict clause from UNSAT proofs

Input: A DNN verification query $Q = \langle V, A, l, u, R \rangle$, a list of lemmas Lem , an UNSAT partial assignment α , and a proof of UNSAT w

Output: A conflict clause of boolean variables

```
1:  $C := proofCC'(Q, \alpha, w)$  ▷ The initial conflict clause
2:  $L := proofLemmas(Q, Lem, w)$  ▷ A queue of lemmas to be analyzed
3: while  $L \neq \emptyset$  do
4:    $w' := L.pop().getProofVector()$ 
5:    $C := C \vee proofCC'(Q, \alpha, w')$ 
6:    $L.enqueue(proofLemmas(Q, Lem, w'))$ 
7: end while
8: return  $C$ 
```

Conceptually, the algorithm deduces the Boolean literals and non-phase-fixing lemmas sufficient for proving UNSAT. The algorithm then recursively analyses the dependency of the lemmas, and adds their clauses to the overall clause. The process is repeated until no non-phase-fixing lemmas are left to be analyzed. To avoid cycles, each lemma is given a unique, chronological ID. Whenever a lemma with ID k is analyzed, only lemmas with ID $l < k$ are considered in the analysis. Our final algorithm appears as Algorithm 3, which uses Algorithm 1 and Algorithm 2 as subroutines.

This algorithm gives rise to an implementation of *T-explain*, by applying it to a proof vector of the lemma, that fixes the phase representing the literal to be explained. We demonstrate these algorithms with an example.

Example 8. Recall that in Example 7, we deduced that $\neg X_3$ is sufficient to derive UNSAT, from a proof vector $w = [0 \ 0 \ -1 \ -2]^\top$. Furthermore, recall that in Example 5, we deduced the phase-fixing lemma $\neg X_3$. For the sake of the example, assume that phase-fixing lemmas are treated as non-phase-fixing lemmas. Therefore, in Algorithm 3, we deduce \emptyset as the initial conflict in line 3, and a single phase fixing lemma as in Example 5 in L, based on the fact that we store it as bounding $u(b_3)$. Then, the vector $w' = [0 \ 0 \ 0 \ -0.5]^\top$ is used to derive the expla-

nation for the lemma, which is $\neg X_3$, negated to be X_3 . The algorithm, in this case, returns X_3 as the conflict clause. When the SAT solver invokes *T-explain* for the deduction of $\neg X_3$ the DNN verifier returns $\neg X_3$. Given $\neg X_3$ and X_3 , the SAT solver deduces the refined conflict clause \emptyset , implying the query is UNSAT.

3.3 Property Clauses

Reasoning about the activations of neurons using the SAT solver opens up the possibility to naturally express complicated properties over the network’s neurons. Currently, such properties could be expressed only as constraints over the network’s internal variables. Since access to these variables is not supported in the VNNLIB standard [30], expressing these properties typically requires modifying the DNN itself by exposing hidden neurons to the output layer. Our approach naturally lends itself to a simpler solution: by exposing the Boolean variables already defined as the interface between the SAT solver and the DNN theory solver, we can express such properties directly as propositional formulas, without requiring any modifications to the network. We hypothesize that for properties with a complex Boolean structure, the performance improvement of our CDCL algorithm will be significant. We examine this hypothesis in Section 5.4.

One prominent type of properties we explore is *Neural Activation Patterns* (NAPs) [43, 47]. A NAP is a set of constraints over the network’s ReLU activations or a subset thereof, restricting them to be either active or inactive. Formally, each NAP is a formula of the form $\bigwedge_{i \in \sigma^+} (b_i \geq 0) \wedge \bigwedge_{j \in \sigma^-} (b_j \leq 0)$, where b_i, b_j are values of indexed neurons of the network, *before* applying the activation function. NAPs often include input and output properties φ_I, φ_O as well. Note that without loss of generality of the definitions in Section 2, NAP properties can be reduced to input-output properties [51].

Using the Boolean abstraction described in Section 3.1, NAPs can be reduced to formulas of the form $\varphi_P := \bigwedge_{i \in \sigma^+} X_i \wedge \bigwedge_{j \in \sigma^-} \neg X_j$. Furthermore, a combination of patterns can be explored as well for greater expressiveness — e.g., queries of the form $\varphi_I \wedge \varphi_P \wedge \varphi_O$, or $\varphi_I \wedge \varphi_{P_1} \wedge \neg \varphi_{P_2} \wedge \varphi_O$. The negation of a NAP, $\neg \varphi_{P_2}$, consists of single clause with possibly multiple literals.

3.4 Algorithmic Optimizations

The modular combination of a SAT solver and a DNN theory solver paves the way for multiple significant optimizations, inspired by the literature in both fields. In particular, we consider the following:

Variable State Independent Decaying Sum (VSIDS) [64]. VSIDS is a common SAT solver heuristic to pick a decision variable. The heuristic is to choose the variable (or literal) that appears most frequently in recently learned clauses. Specifically, each variable is assigned a score, initially computed as the number of appearances in existing conflict clauses. Whenever a new conflict clause is learned, the score of the relevant variables is increased by 1. Once in

every constant number of added clauses, the score can be either halved or reset to 0. This gives greater weight to the most recently derived conflicts.

Restart [70]. Restart is another common SAT heuristic, used to prevent solvers from spending too many resources searching in states that are not beneficial for the overall solution. Once in a while, the solver stops searching for an assignment in its current state, and starts a fresh search from the initial state. Note that the conflict clauses learned by that time are kept, so previous **UNSAT** states will be avoided, and termination is guaranteed. Perhaps the most common heuristic for scheduling restarts is the Luby heuristic [62].

DNN Theory Solver SAT Deduction. In our problem construction, the Boolean part of the query is trivial, and every conflict clause derived originates from a contradiction in the DNN theory solver, or the Boolean processing of such contradictions. Therefore, whenever the DNN theory solver finds a **SAT** assignment that is consistent with the partial assignment discovered by the SAT solver, this assignment necessarily satisfies all conflict clauses. This assignment can then be returned as a **SAT** assignment for the entire query, without waiting for the SAT solver to find a complete satisfying Boolean assignment. In the presence of clauses added externally to the SAT solver (as in Section 3.3), the above-mentioned assumption does not hold. Therefore, in this case, the DNN theory solver first needs to check whether the discovered assignment, which satisfies the linear and piecewise-linear constraints, satisfies the external clauses as well. If so, then this assignment is indeed satisfying, and the verification procedure ends.

Conflict Clause Size Reduction. Inspired by algorithms such as quickX-plain [20, 53, 54], we aim to reduce the size of a learned conflict clause while maintaining its unsatisfiability. We formulate the problem, and our algorithm to reduce clauses’ size in Appendix A.

4 Implementation Details

A key motivation behind our proposed approach is its ability to integrate seamlessly with arbitrary SAT solvers in a modular manner. To maximize modularity, we utilize the IPASIR-UP interface [39, 40], which provides a structured way to connect \mathcal{T} -solvers with SAT solvers within a $\text{DPLL}(\mathcal{T})$ framework. While some SAT solvers already support this interface (e.g., CaDiCaL [17]), to the best of our knowledge, no existing DNN theory solver has implemented it thus far. We summarize here the key adjustments required in a DNN theory solver to support IPASIR-UP.

The IPASIR-UP interface includes several methods, some of which serve as notifications from the SAT solver to the \mathcal{T} -solver, informing it of key events during the SAT-level search process. These include notifications for assigned literals (`notify_assignment()`), backtracking to earlier decision levels (`notify_backtrack()`), and the introduction of new decision levels (`notify_new_decision_level()`). Separate methods function as callbacks, allowing the SAT solver to query the \mathcal{T} -solver for relevant information. These include retrieving literals for propagation (`cb_propagate()`), selecting decision variables (`cb_decide()`), and providing explanatory clauses

for previous propagations (`notify_add_reason_clause_lit()`) or conflicts (`notify_add_external_clause_lit()`).

For a DNN theory solver to be IPASIR-UP compatible and support these methods, we propose to maintain several data structures, including context-dependent ones (inspired by those used in Marabou [81] and CVC5 [11]). These structures ensure that whenever the SAT solver backtracks to an earlier level in the search tree, the data within the DNN theory solver reverts to the state it held at that level. Due to length restrictions, we refer the reader to Appendix B for a detailed discussion of the specific data structures used and an in-depth explanation of each method.

5 Evaluation

To evaluate the performance of our method, we extended the Marabou DNN verifier [81] to support the IPASIR-UP interface, as discussed in Section 4.

The natural baseline to which we compare our implementation is Marabou; and to enable a fair comparison, we disabled some optimizations within Marabou that are not yet compatible with its proof-production mode, and thus currently cannot be integrated into our CDCL algorithm. These optimizations, such as Symbolic Bound Tightening [79] and Parallelization [82], require their own proof construction, which could be combined with the existing mechanism. We refer to the version of Marabou without these optimizations as *Vanilla Marabou*, as opposed to the *Optimized Marabou* version that includes them.

We conducted experiments on three families of benchmarks: (i) a robotic navigation system [4]; (ii) the ACASXU models of aircraft collision avoidance [52]; and (iii) NAP benchmarks, as described in Section 3.3. These benchmarks were selected due to their widespread use as DNN verification benchmarks, their safety-critical nature, and for their diversity. Below we provide additional details on each of the three families of benchmarks.

Robotic Navigation System. This benchmark consists of networks produced via deep reinforcement learning (DRL). We use this benchmark to compare the performance of our implementation, using three different methods for learning conflict clauses: (a) using UNSAT proofs, as in Algorithm 3; (b) using trivial conflict clauses, as in Section 3.1; and (c) using the Gurobi LP solver [48] as a backend engine within Marabou, and its built-in support for producing UNSAT cores. In this method, conflict clauses are produced similarly to Algorithm 1, where instead of checking bound participation in $w^\top \cdot A \cdot V$, we check bound participation in a minimal UNSAT core of the LP found by Gurobi (namely, its *Irreducible Infeasible Subsystem (IIS)*). We compare these methods to Vanilla Marabou.

Airborne Collision Avoidance System (ACASXU). This widely recognized DNN verification benchmark consists of neural networks designed for an airborne collision avoidance system for unmanned aircraft. In our second experiment, we use this benchmark to evaluate the impact of the various optimizations described in Section 3.4. We again use Vanilla Marabou as a baseline.

Neural Activation Patterns (NAP). We use this benchmark to compare our implementation of proof-based CDCL against the state-of-the-art NeuralSAT tool [32], which incorporates its own version of the CDCL algorithm for DNN verification. Here, we also compare performance against the optimized, state-of-the-art version of Marabou. This benchmark is used to evaluate our method for verifying properties with an increasingly complex Boolean structure, as presented in Section 3.3.

5.1 Experimental Setup

All experiments were conducted on CPUs running Linux Debian 12. In the first experiment (robotic navigation system), each query was run on a single CPU with 8GB RAM and 2-hour timeout. In the second experiment (ACASXU), each query was run on a single CPU with 64GB RAM and a 30-hour timeout. Finally, in the third experiment (NAP), each query was run on a single CPU with 64GB RAM and a 2-hour timeout.

5.2 Experiment 1: Comparing Conflict Clause Learning Methods

In this experiment, we evaluate the performance of Marabou with different methods for learning conflict clauses. We used the Robotics benchmark, which contains 2,340 queries: 2,126 satisfiable queries, and 214 unsatisfiable ones. The configurations compared in this experiment were as follows:

- **Vanilla Marabou:** The baseline version.
- **CDCL+Trivial:** Trivial conflict clauses.
- **CDCL+Proof:** Conflict clauses derived from UNSAT proofs.
- **CDCL+Gurobi:** Conflict clauses derived from Gurobi.

All CDCL configurations incorporated VSIDS and Restart optimizations, as these optimizations were empirically observed to be useful (see also Section 5.3).

The results of this experiment are summarized in Table 1. All configurations successfully solved all queries. The data indicate a significant performance improvement when using **CDCL+Proof**, particularly for UNSAT queries. We observe a minor increase in the average solving time for SAT queries compared to Vanilla Marabou when using Marabou’s proof-based conflict clauses; but we deem this to be an acceptable (and unsurprising) increase, given the already fast solving times for these queries — which make the CDCL infrastructure’s overhead more noticeable.

For UNSAT queries, all CDCL configurations demonstrated a substantial performance improvement over the baseline Vanilla Marabou, with the most notable gains observed in the **CDCL+Proof** configuration. These results highlight the effectiveness of incorporating CDCL in solving UNSAT queries.

5.3 Experiment 2: Comparing CDCL Optimizations

In this experiment we evaluate the impact of the different optimizations discussed in Section 3.4. We use the ACASXU benchmark, which is comprised of 45 networks and 4 properties per network, resulting in a total of 180 queries. The configurations compared in this experiment included:

Table 1: Comparing execution times for SAT and UNSAT queries on the Robotics benchmark, using different methods for producing conflict clauses.

Configuration	SAT Avg. Time (s)	UNSAT Avg. Time (s)	Overall Avg. Time (s)
Vanilla Marabou	0.0539	8.2879	0.8069
CDCL+Trivial	0.0936	3.1767	0.3755
CDCL+Gurobi	0.0912	3.0882	0.3652
CDCL+Proof	0.0657	2.3355	0.2732

- **Vanilla Marabou** as the baseline version (as discussed in Section 5.2).
- **CDCL+Proof**, again as discussed in Section 5.2.
- Marabou with proof-based CDCL, enhanced with:
 - **CDCL+Proof+VSIDS**: the VSIDS decision heuristic, combined with Marabou’s existing decision heuristic.
 - **CDCL+Proof+Restart**: the Restart mechanism.
 - **CDCL+Proof+QX**: conflict clause size reduction, discussed in Appendix A.
- **CDCL+Proof+VSIDS+Restart**: Marabou with proof-based CDCL enhanced with both the VSIDS and Restart features.

The results for the ACASXU benchmark are presented in Table 2. Within the time limit, all CDCL configurations successfully solved all queries, whereas **Vanilla Marabou** solved 175 out of 180 queries. Among the evaluated configurations, **CDCL+Proof+ VSIDS+Restart** achieved the best performance. Interestingly, the algorithm to reduce conflict size actually harmed performance.

Table 2: Comparison of execution times on the ACASXU benchmark for different configurations of Marabou. Solving times are averaged over queries solved by all configurations.

Configuration	SAT Avg. Time (s)	UNSAT Avg. Time (s)	Overall Avg. Time (s)
Vanilla Marabou	1114.46	8432.37	6550.63
CDCL+Proof	540.56	3246.03	2550.34
CDCL+Proof+VSIDS	506.37	3222.25	2523.88
CDCL+Proof+Restart	520.59	2926.97	2308.19
CDCL+Proof+QX	539.77	3540.13	2768.61
CDCL+Proof+VSIDS+Restart	464.76	2805.91	2203.90

5.4 Experiment 3: Comparing to Optimized Verifiers

In this experiment, we evaluate the optimal configuration of Marabou enhanced with CDCL, as discovered in 5.3, against the state-of-the-art tool NeuralSAT [32] and the optimized version of Marabou. The evaluation was conducted on the NAP [47] benchmark across four distinct scenarios:

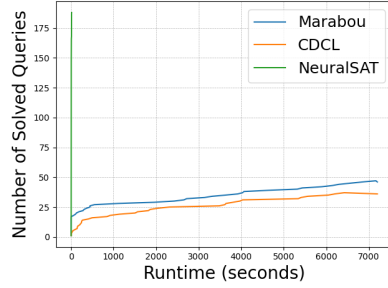
- **Scenario 1:** The original NAP queries introduced in [47], of the form: “given a NAP φ_P of class i , is there a counterexample that satisfies φ_P , but which is not classified as i ?”. This scenario consists of a total of 235 queries.
- **Scenario 2:** Queries of the form: “Given NAPs φ_{P_0} and φ_{P_1} of classes 0 and 1 respectively, is there a counterexample that satisfies $\varphi_{P_0} \wedge \neg\varphi_{P_1}$, and is not classified as 0?”. This scenario includes 76 NAPs of class 0 and 12 NAPs of class 1, resulting in 912 queries in total.
- **Scenario 3:** Queries of the form: “Given NAPs φ_{P_0} , φ_{P_1} , and φ_{P_2} of classes 0, 1, and 2 respectively, is there a counterexample that satisfies $\varphi_{P_0} \wedge \neg\varphi_{P_1} \wedge \neg\varphi_{P_2}$, and is not classified as 0?”. For this scenario, five arbitrary NAPs of class 0 were selected, and queries were generated by pairing them with any of the 12 NAPs of class 1 and 17 NAPs of class 2, resulting in a total of 1,020 queries. Additionally, two versions of this scenario were created: one uses the original input bounds given in [47], and another uses tighter input bounds. This adjustment was made because, during the initial evaluation, all queries in the above scenarios either resulted in **SAT** or timed out. By tightening the bounds, we aimed to include **UNSAT** queries as well, thereby enabling a more comprehensive evaluation.

For Scenarios 2 and 3, the queries were encoded as described in Section 3.3. To enable encoding these queries for NeuralSAT, we modified the relevant ONNX networks by adding new outputs, which correspond to the outputs of the hidden neurons associated with the NAPs.⁴

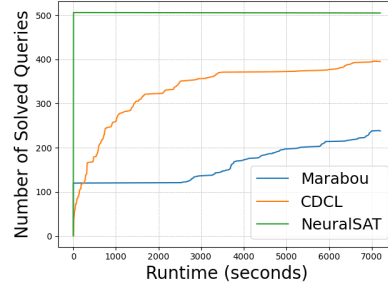
Figure 4 illustrates the runtime comparisons for the three scenarios of the NAP benchmark, including the two variations of Scenario 3. The x-axis represents runtime in seconds, and the y-axis corresponds to the number of solved queries, sorted by runtime for each configuration. In Scenario 1, CDCL exhibits weaker performance compared to NeuralSAT and Marabou. However, in the more complex queries of Scenarios 2 and 3, CDCL demonstrates significant improvements, emphasizing its strength in tackling challenging benchmarks. Upon further analysis of NeuralSAT’s results, we observed that the tool’s quick resolution of queries in Scenarios 1, 2, and 3a was primarily due to the inclusion of an adversarial attack [2] mechanism built into NeuralSAT. Since adversarial attacks are orthogonal to the search process which is our topic here, we also re-evaluated these scenarios with the adversarial attack disabled. This resulted in all queries timing out, or running out of memory, within the defined time and memory limit.

For Scenario 3b, where all queries resulted in **UNSAT**, Marabou demonstrated the best performance. NeuralSAT solved most queries rapidly but required significantly more time for the more complex queries compared to CDCL. Marabou’s superior performance in this scenario suggests room for further enhancement of CDCL. Specifically, we hypothesize that the tightened input bounds enabled Marabou, which supports symbolic bound tightening, to solve these queries more

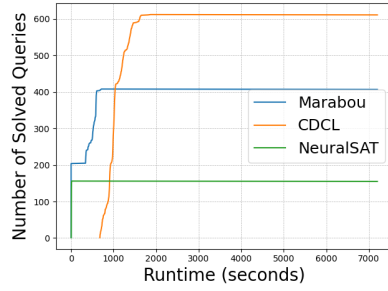
⁴ We attempted to include in the comparison other state-of-the-art tools, such as α - β -CROWN [63, 80] and PyRAT [60]. However, to the best of our knowledge, these tools do not support solving the complex queries required for these scenarios. All tools were considered due to their excellent performance in VNNCOMP 2024 [21].



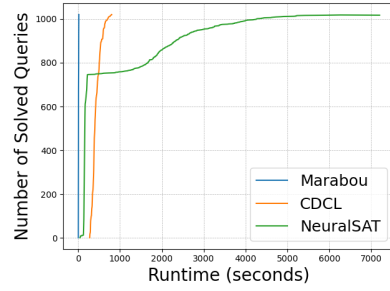
(a) Runtime comparison for Scenario 1.



(b) Runtime comparison for Scenario 2.



(c) Runtime comparison for Scenario 3a.



(d) Runtime comparison for Scenario 3b.

Fig. 4: Runtime comparison for the different scenarios of the experiment.

efficiently than CDCL. Improving Marabou so that these optimizations become compatible with proof production and CDCL could thus boost its performance.

For additional results for this experiment, including the number of solved queries for each verification tool and the average solving time, we refer the reader to Appendix C.

6 Conclusion, Related Work and Future Work

In this work, we introduce a novel algorithm that uses UNSAT proofs and CDCL principles to enhance the scalability of DNN verifiers. Our algorithm is based on a Boolean abstraction of activation functions, and on deriving conflict clauses using UNSAT proofs. We implemented our algorithm using an interface for combining SAT solvers and DNN theory solvers, and evaluated it using diverse benchmarks. Our preliminary results suggest that our algorithm significantly outperforms the baseline DNN verifier, although several of the existing optimizations are not yet compatible with CDCL mode. In specific cases, our algorithm outperforms even highly optimized verifiers.

Related Work There are several DNN verifiers that employ CDCL-like verification schemes [32,33,61], based on the analogy between ReLU phases and Boolean assignments. However, these verifiers use a naive clause learning algorithm; or they employ LP solving to detect UNSAT cases, and then use LP solving again [23] to minimize clause sizes. In contrast, our method uses information from UNSAT proofs to derive a non-trivial conflict clause.

The DNN verification problem can be regarded as a specific case of SMT solving, which would allow using general-purpose, CDCL-based SMT solvers to dispatch DNN verification queries [12]. However, this approach was repeatedly shown to be inefficient [55], and it is currently not used in modern DNN verifiers [21]. Thus, dedicated algorithms and tools for DNN verification are needed.

Previous studies have attempted to analyze dependencies between the phases of neurons as part of the DNN verification process [19]. Such dependencies could be used in generating conflict clauses, and it would be interesting to study the synergies between that approach and the one we propose here.

Future Work Moving forward, we aim to extend our work along several orthogonal paths. First, we intend to extend the CDCL framework to support additional activation functions, such as *maxpool*, *leakyRelu*, and others. Second, we plan to extend this framework to support additional optimizations performed by DNN verifiers, mainly abstract interpretation [63, 75, 80] and parallelization [82] — thus combining the strengths of all these techniques. Third, we aim to explore additional optimizations for SAT solvers’ decision heuristics in the context of DNN verification. We believe that combining these directions will result in a faster and more versatile verifier, which could scale to considerably larger DNNs than is possible today.

Acknowledgments The authors wish to thank Armin Biere, Katalin Fazekas, Mathias Fleury and Mathias Preiner for their helpful advice on SAT and SMT solving; and Divya Gopinath and Corina Pasareanu for their guidance in exploring NAP properties. The work of Isac, Refaeli and Katz was supported by the Binational Science Foundation (grant numbers 2020250 and 2021769), the Israeli Science Foundation (grant number 558/24) and the European Union (ERC, VeriDeL, 101112713). Views and opinions expressed are however those of the author(s) only and do not necessarily reflect those of the European Union or the European Research Council Executive Agency. Neither the European Union nor the granting authority can be held responsible for them. The work of Barrett was supported by in part by the Binational Science Foundation (grant number 2020250), the National Science Foundation (grant numbers 1814369 and 2211505), and the Stanford Center for AI Safety.

References

1. E. Abraham and G. Kremer. SMT Solving for Arithmetic Theories: Theory and Tool Support. In *19th Int. Symposium on Symbolic and Numeric Algorithms for Scientific Computing (SYNASC)*, pages 1–8, 2017.
2. N. Akhtar and A. Mian. Threat of Adversarial Attacks on Deep Learning in Computer Vision: A Survey. *IEEE Access*, 6:14410–14430, 2018.
3. M. Akintunde, A. Kevorchian, A. Lomuscio, and E. Pirovano. Verification of RNN-Based Neural Agent-Environment Systems. In *Proc. 33rd AAAI Conf. on Artificial Intelligence (AAAI)*, pages 197–210, 2019.
4. G. Amir, D. Corsi, R. Yerushalmi, L. Marzari, D. Harel, A. Farinelli, and G. Katz. Verifying Learning-Based Robotic Navigation Systems. In *Proc. 29th Int. Conf. on Tools and Algorithms for the Construction and Analysis of Systems (TACAS)*, pages 607–627, 2023.

5. G. Amir, Z. Freund, G. Katz, E. Mandelbaum, and I. Refaeli. veriFIRE: Verifying an Industrial, Learning-Based Wildfire Detection System. In *Proc. 25th Int. Symposium on Formal Methods (FM)*, pages 648–656, 2023.
6. G. Amir, O. Maayan, T. Zelazny, G. Katz, and M. Schapira. Verifying Generalization in Deep Learning. In *Proc. 35th Int. Conf. on Computer Aided Verification (CAV)*, pages 438–455, 2023.
7. G. Amir, M. Schapira, and G. Katz. Towards Scalable Verification of Deep Reinforcement Learning. In *Proc. 21st Int. Conf. on Formal Methods in Computer-Aided Design (FMCAD)*, pages 193–203, 2021.
8. G. Amir, T. Zelazny, G. Katz, and M. Schapira. Verification-Aided Deep Ensemble Selection. In *Proc. 22nd Int. Conf. on Formal Methods in Computer-Aided Design (FMCAD)*, pages 27–37, 2022.
9. G. Avni, R. Bloem, K. Chatterjee, T. Henzinger, B. Konighofer, and S. Pranger. Run-Time Optimization for Learned Controllers through Quantitative Games. In *Proc. 31st Int. Conf. on Computer Aided Verification (CAV)*, pages 630–649, 2019.
10. T. Baluta, S. Shen, S. Shinde, K. Meel, and P. Saxena. Quantitative Verification of Neural Networks And its Security Applications. In *Proc. 26th ACM Conf. on Computer and Communication Security (CCS)*, 2019.
11. H. Barbosa, C. Barrett, M. Brain, G. Kremer, H. Lachnitt, M. Mann, A. Mohamed, M. Mohamed, A. Niemetz, A. Nötzli, A. Ozdemir, M. Preiner, A. Reynolds, Y. Sheng, C. Tinelli, and Y. Zohar. CVC5: A Versatile and Industrial-Strength SMT Solver. In *Proc. 28th Int. Conf. on Tools and Algorithms for the Construction and Analysis of Systems (TACAS)*, pages 415–442, 2022.
12. H. Barbosa, C. Barrett, B. Cook, B. Dutertre, G. Kremer, H. Lachnitt, A. Niemetz, A. Nötzli, A. Ozdemir, M. Preiner, A. Reynolds, C. Tinelli, and Y. Zohar. Generating and Exploiting Automated Reasoning Proof Certificates. *Communications of the ACM*, 66(10):86–95, 2023.
13. C. Barrett and C. Tinelli. Satisfiability Modulo Theories. In E. Clarke, T. Henzinger, H. Veith, and R. Bloem, editors, *Handbook of Model Checking*, pages 305–343. Springer International Publishing, 2018.
14. S. Bassan, G. Amir, D. Corsi, I. Refaeli, and G. Katz. Formally Explaining Neural Networks within Reactive Systems. In *Proc. 23rd Int. Conf. on Formal Methods in Computer-Aided Design (FMCAD)*, pages 10–22, 2023.
15. S. Bassan and G. Katz. Towards Formal XAI: Formally Approximate Minimal Explanations of Neural Networks. In *Proc. 29th Int. Conf. on Tools and Algorithms for the Construction and Analysis of Systems (TACAS)*, pages 187–207, 2023.
16. R. Bayardo Jr and R. Schrag. Using CSP Look-Back Techniques to Solve Real-World SAT Instances. In *Proc. 14th Nat. Conf. on Artificial Intelligence (AAAI)*, pages 203–208, 1997.
17. A. Biere, T. Faller, K. Fazekas, M. Fleury, N. Froleyks, and F. Pollitt. CaDiCaL 2.0. In *Proc. 36th Int. Conf. on Computer Aided Verification (CAV)*, pages 133–152, 2024.
18. M. Bojarski, D. Del Testa, D. Dworakowski, B. Firner, B. Flepp, P. Goyal, L. Jackel, M. Monfort, U. Muller, J. Zhang, X. Zhang, J. Zhao, and K. Zieba. End to End Learning for Self-Driving Cars, 2016. Technical Report. <http://arxiv.org/abs/1604.07316>.
19. E. Botoeva, P. Kouvaros, J. Kronqvist, A. Lomuscio, and R. Misener. Efficient Verification of ReLU-Based Neural Networks via Dependency Analysis. In *Proc. 34th AAAI Conf. on Artificial Intelligence (AAAI)*, pages 3291–3299, 2020.
20. A. Bradley and Z. Manna. Property-Directed Incremental Invariant Generation. *Formal Aspects of Computing*, 20:379–405, 2008.

21. C. Brix, S. Bak, T. Johnson, and H. Wu. The Fifth International Verification of Neural Networks Competition (VNN-COMP 2024): Summary and Results, 2024. Technical Report. <http://arxiv.org/abs/2412.19985>.
22. C. Brix, M. Müller, S. Bak, T. Johnson, and C. Liu. First Three Years of the International Verification of Neural Networks Competition (VNN-COMP). *Int. Journal on Software Tools for Technology Transfer*, pages 1–11, 2023.
23. J. Chinneck and E. Dravnieks. Locating Minimal Infeasible Constraint Sets in Linear Programs. *ORSA Journal on Computing*, 3(2):157–168, 1991.
24. V. Chvátal. *Linear Programming*. W. H. Freeman and Company, 1983.
25. E. Cohen, Y. Elboher, C. Barrett, and G. Katz. Tighter Abstract Queries in Neural Network Verification. In *Proc. 24th Int. Conf. on Logic for Programming, Artificial Intelligence and Reasoning (LPAR)*, pages 124–143, 2023.
26. G. Dantzig. *Linear Programming and Extensions*. Princeton University Press, 1963.
27. M. Davis, G. Logemann, and D. Loveland. A Machine Program for Theorem-Proving. *Communications of the ACM*, 5(7):394–397, 1962.
28. M. Davis and H. Putnam. A Computing Procedure for Quantification Theory. *Journal of the ACM (JACM)*, 7(3):201–215, 1960.
29. L. de Moura and N. Bjørner. Satisfiability Modulo Theories: Introduction and Applications. *Communications of the ACM*, 54(9):69–77, 2011.
30. S. Demarchi, D. Guidotti, L. Pulina, and A. Tacchella. Supporting Standardization of Neural Networks Verification with VNNLIB and CoCoNet. In *Proc. 6th Int. Workshop on Formal Methods for ML-Enabled Autonomous Systems (FoMLAS)*, pages 47–58, 2023.
31. N. Dershowitz, Z. Hanna, and A. Nadel. A Scalable Algorithm for Minimal Unsatisfiable Core Extraction. In *Proc. 9th Int. Conf. on Theory and Applications of Satisfiability Testing (SAT)*, pages 36–41, 2006.
32. H. Duong, T. Nguyen, and M. Dwyer. A DPLL(T) Framework for Verifying Deep Neural Networks, 2023. Technical Report. <http://arxiv.org/abs/2307.10266>.
33. R. Ehlers. Formal Verification of Piece-Wise Linear Feed-Forward Neural Networks. In *Proc. 15th Int. Symp. on Automated Technology for Verification and Analysis (ATVA)*, pages 269–286, 2017.
34. Y. Elboher, E. Cohen, and G. Katz. Neural Network Verification using Residual Reasoning. In *Proc. 20th Int. Conf. on Software Engineering and Formal Methods (SEFM)*, pages 173–189, 2022.
35. Y. Elboher, E. Cohen, and G. Katz. On Applying Residual Reasoning within Neural Network Verification. *Int. Journal on Software and Systems Modeling (SoSyM)*, 2023.
36. Y. Elboher, R. Elsaleh, O. Isac, M. Ducoffe, A. Galametz, G. Pováda, R. Boumazouza, N. Cohen, and G. Katz. Robustness Assessment of a Runway Object Classifier for Safe Aircraft Taxiing. In *Proc. 43rd Int. Digital Avionics Systems Conf. (DASC)*, 2024.
37. Y. Elboher, J. Gottschlich, and G. Katz. An Abstraction-Based Framework for Neural Network Verification. In *Proc. 32nd Int. Conf. on Computer Aided Verification (CAV)*, pages 43–65, 2020.
38. T. Eliyahu, Y. Kazak, G. Katz, and M. Schapira. Verifying Learning-Augmented Systems. In *Proc. Conf. of the ACM Special Interest Group on Data Communication on the Applications, Technologies, Architectures, and Protocols for Computer Communication (SIGCOMM)*, pages 305–318, 2021.
39. K. Fazekas, A. Niemetz, M. Preiner, M. Kirchweiger, S. Szeider, and A. Biere. IPASIR-UP: User Propagators for CDCL. In *Proc. 26th Int. Conf. on Theory and Applications of Satisfiability Testing (SAT)*, pages 1–13, 2023.

40. K. Fazekas, A. Niemetz, M. Preiner, M. Kirchweger, S. Szeider, and A. Biere. Satisfiability Modulo User Propagators. *Journal of Artificial Intelligence Research*, 81:989–1017, 2024.
41. H. Ganzinger, G. Hagen, R. Nieuwenhuis, A. Oliveras, and C. Tinelli. DPLL (T): Fast Decision Procedures. In *Proc. 16th Int. Conf. on Computer Aided Verification (CAV)*, pages 175–188, 2004.
42. T. Gehr, M. Mirman, D. Drachler-Cohen, E. Tsankov, S. Chaudhuri, and M. Vechev. AI2: Safety and Robustness Certification of Neural Networks with Abstract Interpretation. In *Proc. 39th IEEE Symposium on Security and Privacy (S&P)*, 2018.
43. C. Geng, N. Le, X. Xu, Z. Wang, A. Gurfinkel, and X. Si. Towards Reliable Neural Specifications. In *Proc. Int. Conf. on Machine Learning (ICML)*, pages 11196–11212, 2023.
44. S. Gokulanathan, A. Feldsher, A. Malca, C. Barrett, and G. Katz. Simplifying Neural Networks using Formal Verification. In *Proc. 12th NASA Formal Methods Symposium (NFM)*, pages 85–93, 2020.
45. B. Goldberger, Y. Adi, J. Keshet, and G. Katz. Minimal Modifications of Deep Neural Networks using Verification. In *Proc. 23rd Int. Conf. on Logic for Programming, Artificial Intelligence and Reasoning (LPAR)*, pages 260–278, 2020.
46. I. Goodfellow, Y. Bengio, and A. Courville. *Deep Learning*. MIT Press, 2016.
47. D. Gopinath, H. Converse, C. Pasareanu, and A. Taly. Property Inference for Deep Neural Networks. In *Proc. 34th IEEE/ACM Int. Conf. on Automated Software Engineering (ASE)*, pages 797–809, 2019.
48. The Gurobi Optimizer. <https://www.gurobi.com/>.
49. X. Huang, M. Kwiatkowska, S. Wang, and M. Wu. Safety Verification of Deep Neural Networks. In *Proc. 29th Int. Conf. on Computer Aided Verification (CAV)*, pages 3–29, 2017.
50. O. Isac, C. Barrett, M. Zhang, and G. Katz. Neural Network Verification with Proof Production. In *Proc. 22nd Int. Conf. on Formal Methods in Computer-Aided Design (FMCAD)*, pages 38–48, 2022.
51. O. Isac, Y. Zohar, C. Barrett, and G. Katz. DNN Verification, Reachability, and the Exponential Function Problem. In *Proc. 34th Int. Conf. on Concurrency Theory (CONCUR)*, 2023.
52. K. Julian, M. Kochenderfer, and M. Owen. Deep Neural Network Compression for Aircraft Collision Avoidance Systems. *Journal of Guidance, Control, and Dynamics*, 42(3):598–608, 2019.
53. U. Junker. Quickxplain: Conflict Detection for Arbitrary Constraint Propagation Algorithms. In *Proc. Workshop on Modelling and Solving Problems with Constraints*, 2001.
54. U. Junker. Quickxplain: Preferred Explanations and Relaxations for Over-Constrained Problems. In *Proc. 19th Nat. Conf. on Artificial Intelligence (AAAI)*, pages 167–172, 2004.
55. G. Katz, C. Barrett, D. Dill, K. Julian, and M. Kochenderfer. Reluplex: a Calculus for Reasoning about Deep Neural Networks. *Formal Methods in System Design (FMSD)*, 2021.
56. G. Katz, D. Huang, D. Ibeling, K. Julian, C. Lazarus, R. Lim, P. Shah, S. Thakoor, H. Wu, A. Zeljić, D. Dill, M. Kochenderfer, and C. Barrett. The Marabou Framework for Verification and Analysis of Deep Neural Networks. In *Proc. 31st Int. Conf. on Computer Aided Verification (CAV)*, pages 443–452, 2019.
57. Y. Kazak, C. Barrett, G. Katz, and M. Schapira. Verifying Deep-RL-Driven Systems. In *Proc. 1st ACM SIGCOMM Workshop on Network Meets AI & ML (NetAI)*, pages 83–89, 2019.

58. P. Kouvaros, F. Leofante, B. Edwards, C. Chung, D. Margineantu, and A. Lomuscio. Verification of Semantic Key Point Detection for Aircraft Pose Estimation. In *Proc. 20th Int. Conf. on Principles of Knowledge Representation and Reasoning (KR)*, pages 757–762, 2023.
59. O. Lahav and G. Katz. Pruning and Slicing Neural Networks using Formal Verification. In *Proc. 21st Int. Conf. on Formal Methods in Computer-Aided Design (FMCAD)*, pages 183–192, 2021.
60. A. Lemesle, J. Lehmann, and T. Gall. Neural Network Verification with PyRAT, 2024. Technical Report. <http://arxiv.org/abs/2410.23903>.
61. Z. Liu, P. Yang, L. Zhang, and X. Huang. DeepCDCL: A CDCL-based Neural Network Verification Framework. In *Proc. 18th Int. Symposium on Theoretical Aspects of Software Engineering (TASE)*, pages 343–355, 2024.
62. M. Luby, A. Sinclair, and D. Zuckerman. Optimal Speedup of Las Vegas Algorithms. *Information Processing Letters*, 47(4):173–180, 1993.
63. Z. Lyu, C.-Y. Ko, Z. Kong, N. Wong, D. Lin, and L. Daniel. Fastened Crown: Tightened Neural Network Robustness Certificates. In *Proc. 34th AAAI Conf. on Artificial Intelligence (AAAI)*, pages 5037–5044, 2020.
64. M. Moskewicz, C. Madigan, Y. Zhao, L. Zhang, and S. Malik. Chaff: Engineering an Efficient SAT Solver. In *Proc. 38th Annual Design Automation Conference (DAC)*, pages 530–535, 2001.
65. M. Müller, G. Makarchuk, G. Singh, M. Püschel, and M. Vechev. PRIMA: General and Precise Neural Network Certification via Scalable Convex Hull Approximations. In *Proc. 49th ACM SIGPLAN Symposium on Principles of Programming Languages (POPL)*, 2022.
66. G. Nelson and D. Oppen. Simplification by Cooperating Decision Procedures. *ACM Transactions on Programming Languages and Systems (TOPLAS)*, 1(2):245–257, 1979.
67. OpenAI. ChatGPT. <https://chatgpt.com>.
68. L. Pulina and A. Tacchella. An Abstraction-Refinement Approach to Verification of Artificial Neural Networks. In *Proc. 22nd Int. Conf. on Computer Aided Verification (CAV)*, pages 243–257, 2010.
69. P. Rajpurkar, E. Chen, O. Banerjee, and E. J. Topol. AI in Health and Medicine. *Nature Medicine*, 28(1):31–38, 2022.
70. A. Ramos, P. Van Der Tak, and M. Heule. Between Restarts and Backjumps. In *Proc. 14th Int. Conf. on Theory and Applications of Satisfiability Testing (SAT)*, pages 216–229, 2011.
71. I. Refaeli and G. Katz. Minimal Multi-Layer Modifications of Deep Neural Networks. In *Proc. 5th Workshop on Formal Methods for ML-Enabled Autonomous Systems (FoMLAS)*, pages 46–66, 2022.
72. S. Sankaranarayanan, S. Dutta, and S. Mover. Reaching Out Towards Fully Verified Autonomous Systems. In *Proc. 13th Int. Conf. on Reachability Problems (RP)*, pages 22–32, 2019.
73. J. Silva and K. Sakallah. GRASP-A New Search Algorithm for Satisfiability. In *Proc. 15th Int. Conf. on Computer Aided Design (ICCAD)*, pages 220–227, 1996.
74. J. M. Silva and K. A. Sakallah. GRASP: A Search Algorithm for Propositional Satisfiability. *IEEE Transactions on Computers*, 48(5):506–521, 1999.
75. G. Singh, T. Gehr, M. Puschel, and M. Vechev. An Abstract Domain for Certifying Neural Networks. In *Proc. 46th ACM SIGPLAN Symposium on Principles of Programming Languages (POPL)*, 2019.
76. C. Szegedy, W. Zaremba, I. Sutskever, J. Bruna, D. Erhan, I. Goodfellow, and R. Fergus. Intriguing Properties of Neural Networks, 2013. Technical Report. <http://arxiv.org/abs/1312.6199>.

77. V. Tjeng, K. Xiao, and R. Tedrake. Evaluating Robustness of Neural Networks with Mixed Integer Programming, 2017. Technical Report. <http://arxiv.org/abs/1711.07356>.
78. H.-D. Tran, S. Bak, W. Xiang, and T. Johnson. Verification of Deep Convolutional Neural Networks Using ImageStars. In *Proc. 32nd Int. Conf. on Computer Aided Verification (CAV)*, pages 18–42, 2020.
79. S. Wang, K. Pei, J. Whitehouse, J. Yang, and S. Jana. Formal Security Analysis of Neural Networks using Symbolic Intervals. In *Proc. 27th USENIX Security Symposium*, pages 1599–1614, 2018.
80. S. Wang, H. Zhang, K. Xu, X. Lin, S. Jana, C.-J. Hsieh, and Z. Kolter. Beta-Crown: Efficient Bound Propagation with Per-Neuron Split Constraints for Neural Network Robustness Verification. *Advances in Neural Information Processing Systems*, 34:29909–29921, 2021.
81. H. Wu, O. Isac, A. Zeljić, T. Tagomori, M. Daggitt, W. Kokke, I. Refaeli, G. Amir, K. Julian, S. Bassan, P. Huang, O. Lahav, M. Wu, M. Zhang, E. Komendantskaya, G. Katz, and C. Barrett. Marabou 2.0: A Versatile Formal Analyzer of Neural Networks. In *Proc. 36th Int. Conf. on Computer Aided Verification (CAV)*, 2024.
82. H. Wu, A. Ozdemir, A. Zeljic, K. Julian, A. Irfan, D. Gopinath, S. Fouladi, G. Katz, C. Pasareanu, and C. Barrett. Parallelization Techniques for Verifying Neural Networks. In *Proc. 20th Int. Conf. on Formal Methods in Computer-Aided Design (FMCAD)*, pages 128–137, 2020.
83. H. Wu, A. Zeljić, K. Katz, and C. Barrett. Efficient Neural Network Analysis with Sum-of-Infeasibilities. In *Proc. 28th Int. Conf. on Tools and Algorithms for the Construction and Analysis of Systems (TACAS)*, pages 143–163, 2022.
84. H. Zhang, M. Shinn, A. Gupta, A. Gurfinkel, N. Le, and N. Narodytska. Verification of Recurrent Neural Networks for Cognitive Tasks via Reachability Analysis. In *Proc. 24th European Conf. on Artificial Intelligence (ECAI)*, pages 1690–1697, 2020.

Appendix

A Reducing Size of Conflict Clauses

Consider a satisfiable set of constraints B , and a clause C such that $B \wedge C$ is UNSAT. An UNSAT core of $B \wedge C$ is a subset of the constraints $B \wedge C$ that is UNSAT [31]. In particular, we are interested in UNSAT cores of the form $B \wedge C'$ where C' is a subclause of C , $B \wedge C'$ is UNSAT, and for each proper subclause C'' , we have that $B \wedge C''$ is SAT, i.e., C' is *minimal*. The motivation for finding UNSAT cores is that smaller conflict clauses tend to prune large subspaces from the search procedure, and thus improve performance.

There exist several algorithms to find an UNSAT core of a conflict clause [20] such as *quickXplain* [53, 54]. These algorithms typically use binary search to attempt to eliminate literals from the clause. Each time the candidate conflict is checked for inconsistency, typically by attempting to solve a new query constructed from a formula and the candidate clause. If the candidate leads to an UNSAT result, it is kept, and the algorithm attempts to eliminate additional literal. If it leads to SAT, the previously eliminated literals are re-added to the clause. Literals in the clause can also be heuristically ordered, so that “important” literals are eliminated last [54]. If the method for checking candidate conflicts is sound and complete, then the algorithm is guaranteed to find an UNSAT core.

In the context of DNN verification, consider the linear query $\langle A, l, u \rangle$ as our base formula B , and a conflict clause C . We propose an algorithm to reduce the size of conflict clauses, using UNSAT proof vectors w . The most straightforward way to check whether a candidate clause contradicts the given formula is to run a separate verification query; but this can be quite expensive. Instead, we propose a novel *incomplete* but faster method (inspired by [20]): we erase some literals from the clause, and check whether the proof of unsatisfiability we had earlier obtained for the original clause also constitutes a proof of unsatisfiability for the candidate clause. This is done by generating the linear combination $w^\top \cdot A \cdot V$, and updating l, u using the bounds of the ReLU phases given by the literals of the candidate clause. w proves UNSAT for the candidate clause if and only if $w^\top \cdot A \cdot V$ sums to a negative constant, given the updated bounds. Generally, the cost of checking a proof is significantly smaller than that of running an additional query, and so if we are fortunate, we can quickly decide to keep the candidate clause. It is possible, however, that this incomplete method would mistakenly conclude that a candidate is not a conflict clause, when in fact it is one — ultimately leading to non-minimal conflict clauses.

To make this approach more efficient, we order the literals in each clause chronologically, by the decision level in which they were added, and remove the later literals first. By that, we aim for clauses that would prune the search tree in shallower depths.

We formalize the clause minimization algorithm in Algorithm 4, and the checking algorithm in Algorithm 5. Conceptually, Algorithm 4 attempts to eliminate literals from the right half of the clause (higher decision levels). If it suc-

Algorithm 4 *reduceClause()*: Reduce conflict clauses' size using UNSAT proofs

Input: A DNN verification query Q , a proof of UNSAT w , a candidate clause C and a support clause D

Output: A conflict sub-clause of C

```

1: if  $|C| \leq 1$  then
2:   return  $C$ 
3: end if
4:  $C := sortByDecisionLevel(C)$ 
   // Let  $\ell_1 \vee \dots \vee \ell_n$  denote the literals in  $C$ 
5:  $C_1 := \ell_1 \vee \dots \vee \ell_{\lfloor \frac{n}{2} \rfloor}$ ,  $C_2 := \ell_{\lfloor \frac{n}{2} \rfloor + 1} \vee \dots \vee \ell_n$ 
6: if checkClauseProof( $Q, w, D \cup C_1$ ) then
7:   return reduceClause( $Q, w, C_1, D$ )
8: end if
9:  $S_1 := reduceClause(Q, w, C_2, D \cup C_1)$ 
10:  $S_2 := reduceClause(Q, w, C_1, D \cup S_1)$ 
11: return  $S_1 \cup S_2$ 

```

ceeds, it then tries to eliminate literals from the left half of the clause. A literal is eliminated based on Algorithm 5. The latter algorithm fixes the phases of the ReLU constraints, given by the literals in C . Then, the algorithm checks whether the proof vector w attests to UNSAT as in Theorem 1.

Algorithm 5 *checkClauseProof()*: Check conflict of given UNSAT proof and clause

Input: A DNN verification query Q , a proof of UNSAT w and a candidate clause C

Output: \top iff w can prove the UNSAT given the phases of C .

```

   // Let  $\sum_{i=1}^n c_i \cdot x_i$  denote the linear combination of variables in  $w^\top \cdot A \cdot V$ 
1: for  $\ell_j \in C$  do
2:    $x_{j_1} := b_j$ ,  $x_{j_2} := f_j$ 
3:   if  $\ell_j = X_j$  then
4:      $l(x_{j_1}) := 0$ 
5:   else
6:      $u(x_{j_1}) := 0$ ,  $u(x_{j_2}) := 0$ 
7:   end if
8: end for
9: return  $\top$  if and only if  $\sum_{c_i > 0} c_i \cdot u(x_i) + \sum_{c_i < 0} c_i \cdot l(x_i) < 0$ 

```

B Implementation Details of IPASIR-UP Methods

The IPASIR-UP interface includes a *callback* mechanism, in which the SAT solver sends requests to the \mathcal{T} -solver, and a *notification* mechanism, in which the SAT solver updates the \mathcal{T} -solver with information. To properly implement this interface, we manage several internal data structures on the DNN theory solver side. These data structures include a map representing the Boolean abstraction (**satSolverVarToPlc**), a list of deduced literals pending propagation to the SAT solver (**literalsToPropagate**), a context-dependent list of currently assigned literals (**assignedLiterals**), and another context-dependent list of satisfied clauses in the current context. Below, we describe the implementation of each method:

```
void notify_assignment(const std::vector<int> &lits)
```

This method processes a list of literals **lits** assigned by the SAT solver, notifying the theory solver accordingly. The implementation iterates over each literal **lit** in **lits**. For each literal, **lit** is added to the internal list **assignedLiterals**. Subsequently, the corresponding piecewise-linear constraint (**plc**) is retrieved from **satSolverVarToPlc**. The phase of **plc** is fixed based on the sign of **lit**, which may lead to further tightening of bounds for other variables. Finally, the internal list **satisfiedClauses** is updated.

```
void notify_new_decision_level()
```

This method is used to preserve the current state in context-dependent data structures. Specifically, it stores the current lists of assigned literals (**assignedLiterals**) and satisfied clauses (**satisfiedClauses**) into their designated data structures, ensuring consistency across decision levels.

```
void notify_backtrack(size_t new_level)
```

This method facilitates backtracking to the specified decision level **new_level**. It restores the internal state of all context-dependent structures to align with the state corresponding to the given decision level. Specifically, this includes reverting the lists of assigned literals (**assignedLiterals**) and satisfied clauses (**satisfiedClauses**) to their respective states at **new_level**.

```
bool cb_check_found_model(const std::vector<int> &model)
```

This method verifies whether the complete boolean assignment **model**, provided by the SAT solver, satisfies all constraints encoded in the \mathcal{T} -solver. The implementation first applies the functionality described in **notify_assignment** to process each previously unassigned literal in **model**. Following this, the \mathcal{T} -solver is invoked to determine the satisfiability of the constraints imposed by **model**. If the \mathcal{T} -solver identifies a satisfying assignment for all variables under the phase fixings defined by **model**, the method returns **true**. Conversely, if the \mathcal{T} -solver concludes that no such satisfying assignment exists, the method returns **false**.

```
int cb_decide()
```

This method is invoked by the SAT solver to determine the next decision literal. The implementation integrates the VSIDS decision heuristic with other

existing heuristics. A score is computed for each literal based on the applied decision heuristic, and the literal with the highest score is selected. The selected literal is then returned as the decision literal.

int cb.propagate()

This method is invoked by the SAT solver to request additional literals for assignment that may have been deduced by the theory solver. The implementation begins by checking whether the list of pending literals for propagation, `literalsToPropagate`, is empty. If `literalsToPropagate` is empty, the \mathcal{T} -solver is executed to deduce new phase fixings, which are then added to `literalsToPropagate` for subsequent propagation.

The method is repeatedly called to retrieve one literal for propagation at a time until no further literals remain. For each invocation, a single literal from `literalsToPropagate` is propagated. When `literalsToPropagate` becomes empty, the method signals this to the SAT solver by returning 0. Subsequent invocations of `cb.propagate()` will repeat this process, ensuring that all newly deduced literals are propagated until no further deductions are possible.

int cb.add_reason_clause_lit(int propagated_lit)

This method requests a reason clause from the \mathcal{T} -solver, providing an explanation for the previously propagated literal `propagated_lit`. Similar to the process described in `cb.propagate`, the reason clause is constructed and propagated one literal at a time. The end of the clause is signaled by returning 0. The methodology for constructing the reason clause follows the approach outlined in Section 3.2.

bool cb.has_external_clause() / int cb.add_external_clause_lit()

These two methods are used to handle conflict clauses. `cb.has_external_clause()` checks whether a conflict clause was deduced by the \mathcal{T} -solver and is ready for propagation. If a conflict clause is available, `cb.add_external_clause_lit()` propagates one literal from the conflict clause at a time. The end of the conflict clause is signaled by returning 0. The approach for constructing conflict clauses adheres to the methodology described in Section 3.2.

C Additional Results for Experiment 3

In this Appendix, we provide more detailed results for our third experiment, as described in Section 5.4. Recall that NeuralSAT without the adversarial attack was unable to solve any of the SAT queries, i.e., the queries of scenarios 1, 2, and 3a, as all such queries timed out. Therefore, the reported solving times for NeuralSAT are based solely on the performance of the adversarial attack, which can be considered independently of the verification algorithm. Additionally, the solving times reported below are averaged over the number of queries each tool successfully solved. However, due to the variability in the number of queries solved by each tool, a simple average is less informative compared to the first two experiments. The results are summarized in a table for each scenario:

Table 3: Comparison of execution times on Scenario 1 of the NAP benchmark. The result of all solved queries, for all tools, is SAT.

Configuration	# Solved Queries	Avg. Time (s)
CDCL	37	2006.33
Marabou	47	1917.63
NeuralSAT	188	3.64

Table 4: Comparison of execution times on Scenario 2 of the NAP benchmark. The result of all solved queries, for all tools, is SAT.

Configuration	# Solved Queries	Avg. Time (s)
CDCL	396	1149.78
Marabou	239	239.74
NeuralSAT	506	3.13

Table 5: Comparison of execution times on Scenario 3a of the NAP benchmark. The result of all solved queries, for all tools, is SAT.

Configuration	# Solved Queries	Avg. Time (s)
CDCL	612	1044.07
Marabou	408	253.30
NeuralSAT	156	6.14

Table 6: Comparison of execution times on Scenario 3b of the NAP benchmark. The result of all solved queries, for all tools, is UNSAT.

Configuration	# Solved Queries	Avg. Time (s)
CDCL	1020	429.90
Marabou	1020	9.99
NeuralSAT	1018	766.38